

Fig.1 SEM Micrographs of Concrete Specimens Incorporating HDPE as Aggregate Alternative (Adapted from [Syed Nasir Abbas et al., 2024](#))

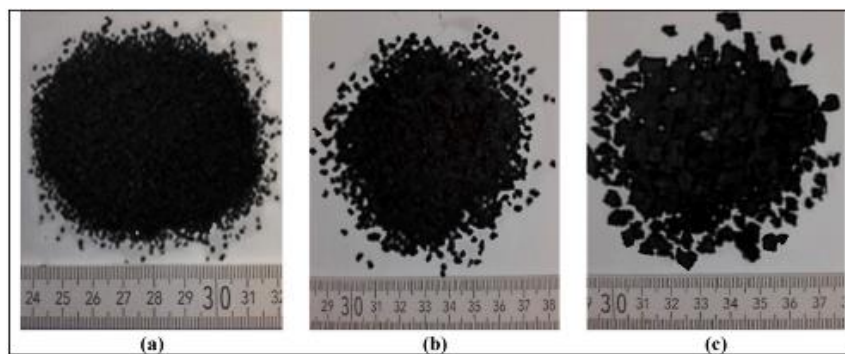


Fig.2 Rubber tire sizes are (a) #10, (b) #3/16, and (c) #3/8. Adapted from [Mohammed A. Al-Osta et al., \(2021\)](#)

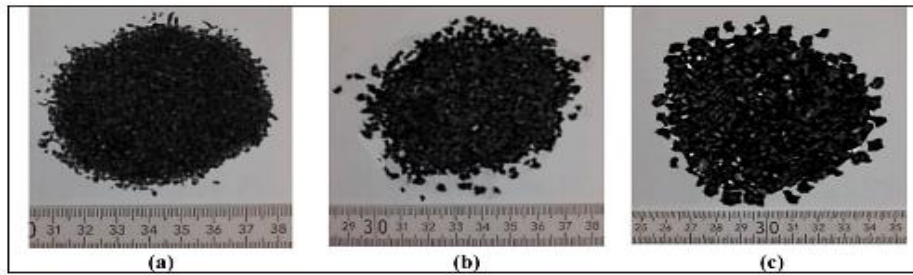


Fig.3 Sizes of HDPE: (a) Fine (#10); (b) coarse (#3/16); (c) coarse (#3/8). Adapted from [Mohammed A. Al-Osta et al., \(2021\)](#)

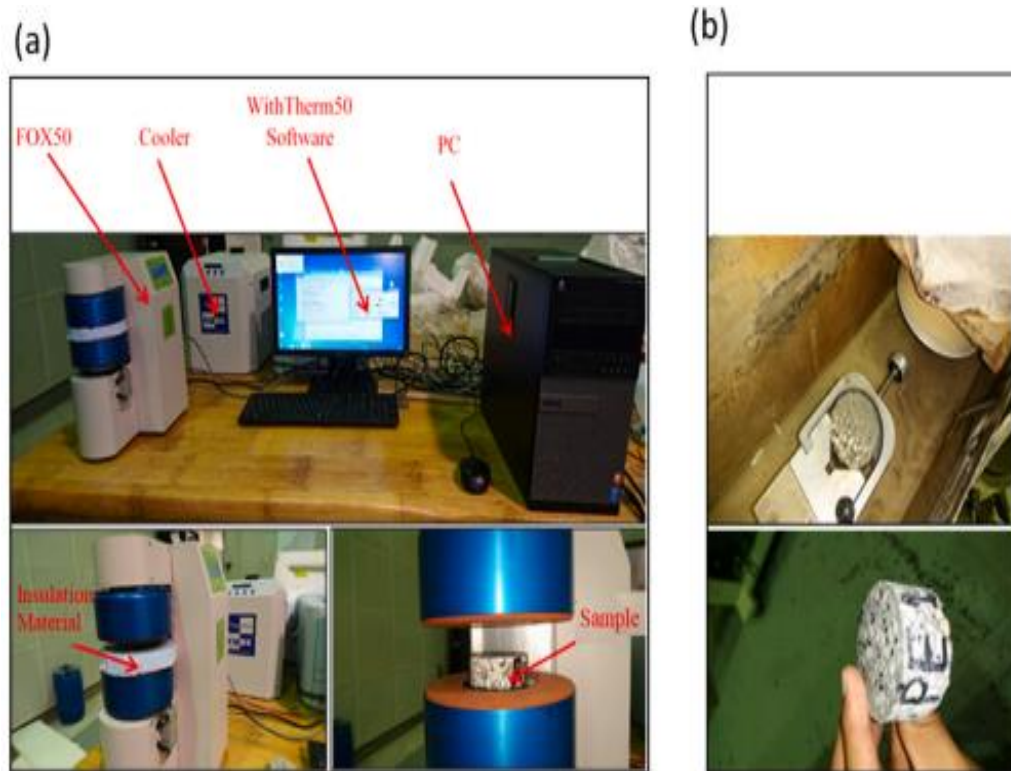


Fig.4 (a) FOX50 Heat Flow Meter Device Setup, (b) Polished Specimen from Both Surfaces. Adapted from [Mohammed A. Al-Osta et al., 2021](#)



Fig.5 Failure Modes of Compressive Strength (CS). Adapted from [Mohammed A. Al-Osta et al., 2021](#)

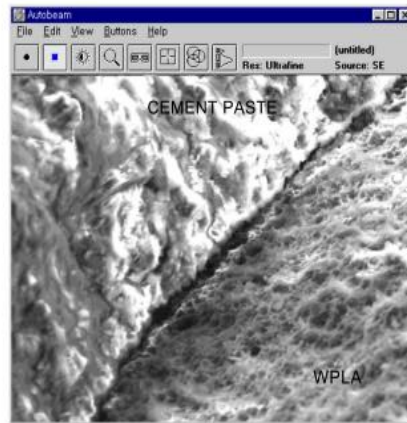


Fig.6 Zone of Transition in Mortar Between WPLA and Cement Paste (28 Days, Magnified x700). Adapted from [Yun-Wang Choi et al., 2004](#)

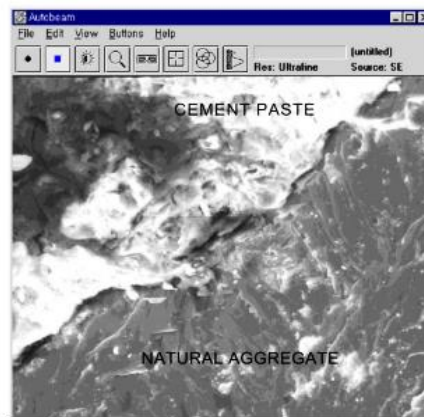


Fig.7 Zone of Transition in Mortar Between Natural Aggregate and Cement Paste (28 Days, Magnified x700). Adapted from [Yun-Wang Choi et al., 2004](#)



Fig.8 Shows the surface microstructure of WPLA in mortar after three and twenty-eight days, magnified by 2000. Adapted from [Yun-Wang Choi et al., 2004](#)

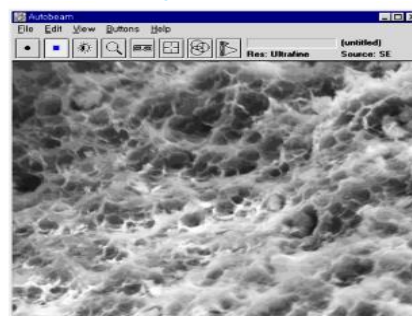


Fig.9 WPLA Surface Microstructure in Mortar (28 Days, x2000 Magnification). Adapted from [Yun-Wang Choi et al., 2004](#)





Fig.10 (a) PET waste following shredding, (b) Using PET in part to prepare a concrete sample. Adapted from [Lukman Abubakar et al., 2024](#)

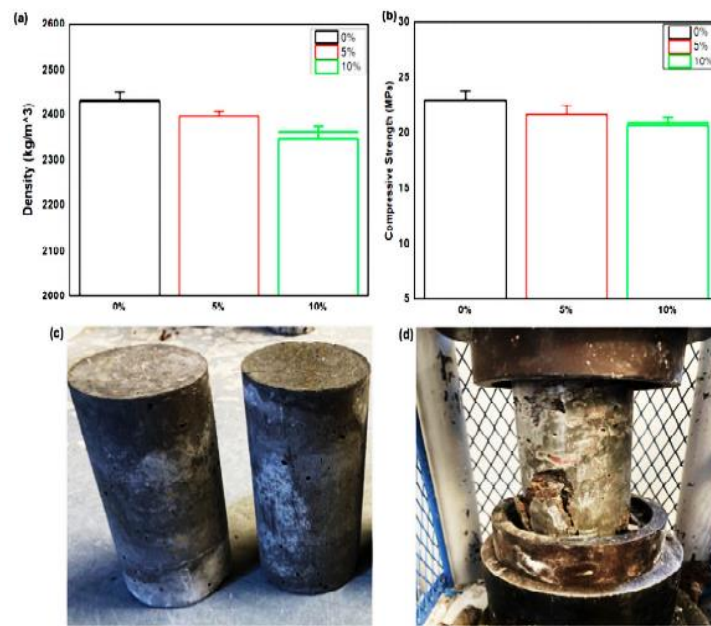


Fig.11 (a) concrete samples' density plot, (b) compressive strength plot, and (c,d) pictures of the concrete samples before and after they failed the compression test. Adapted from [Lukman Abubakar et al., 2024](#)

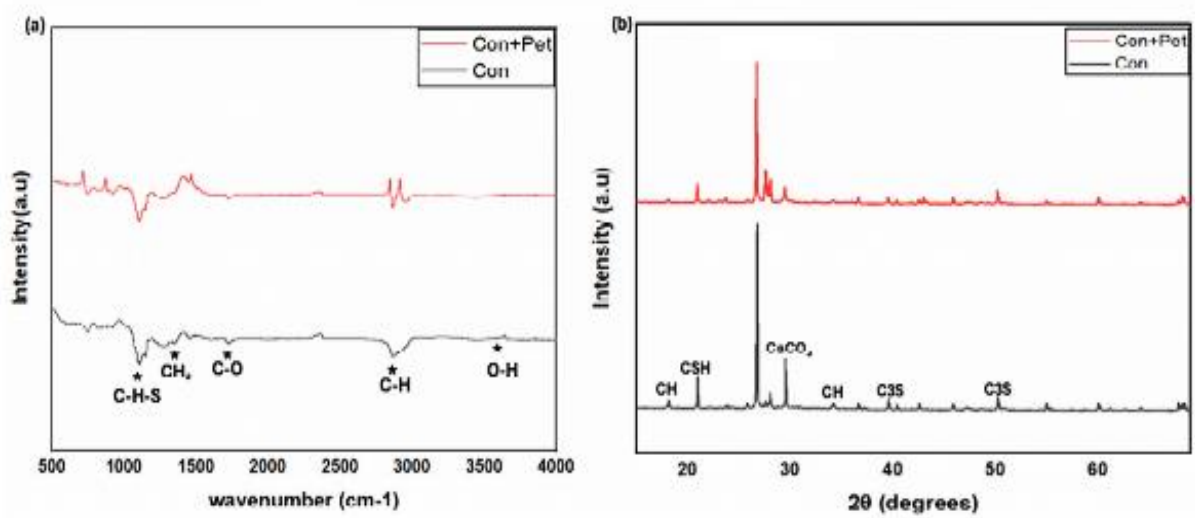


Fig.12 (a) The FTIR and XRD plots of concrete and concrete + PET and concrete both. Adapted from [Lukman Abubakar et al., 2024](#)

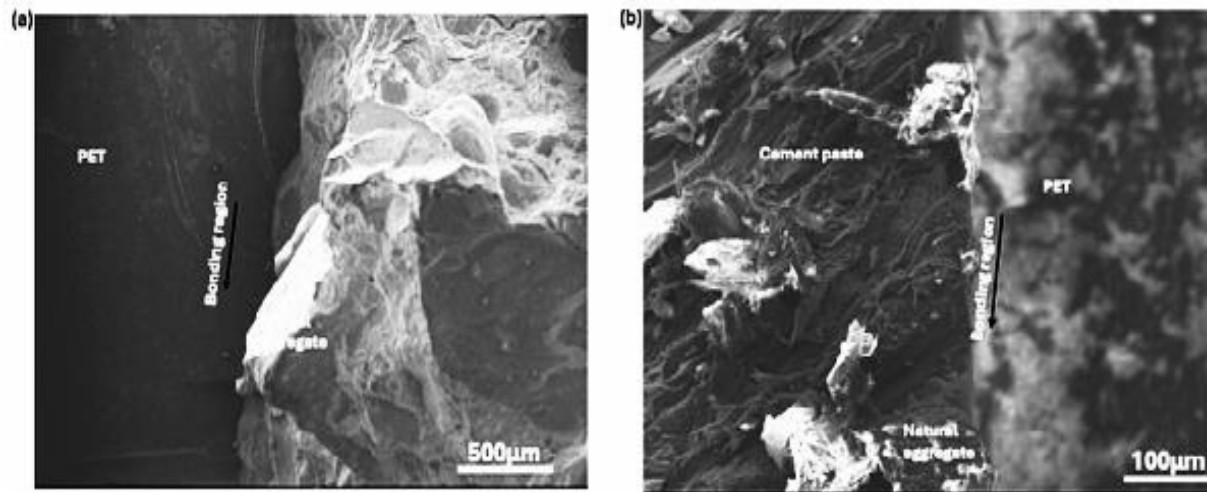


Fig.13 PET aggregate in concrete matrix as shown in SEM photos. Adapted from Lukman [Abubakar et al., 2024](#)



Fig.14 PET coarse aggregate. Adapted from [Md. Jahidul Islam et al.,2016](#)

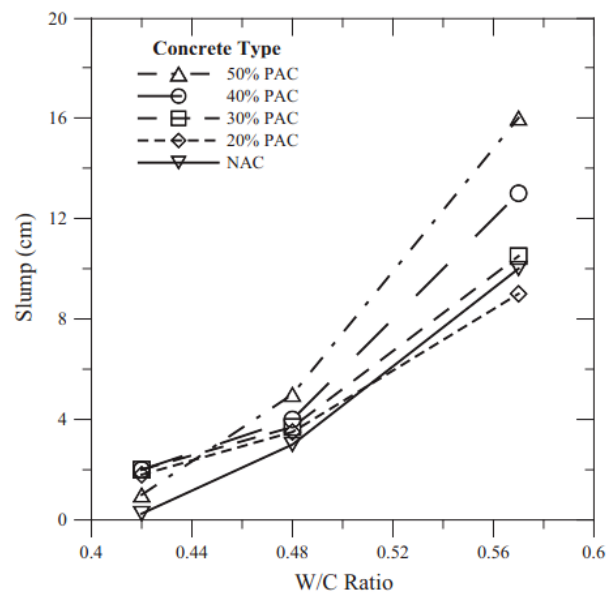


Fig.15 Slump values for various concrete type. Adapted from [Md. Jahidul Islam et al.,2016](#)

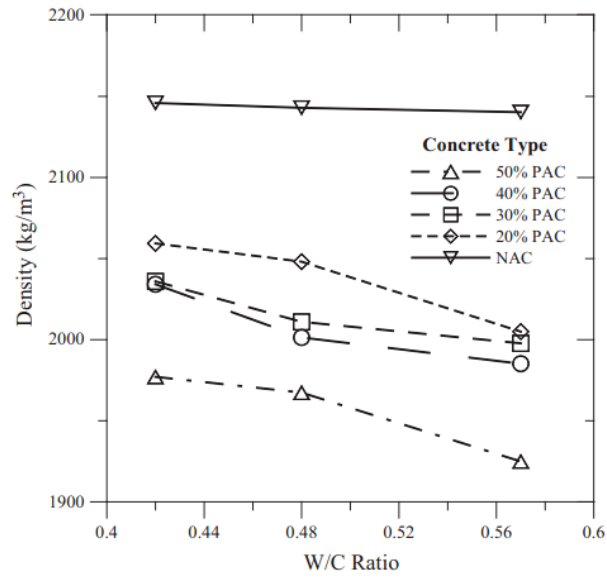


Fig.16 Density variation with w/c ratio for different types of concrete. Adapted from [Md. Jahidul Islam et al.,2016](#)

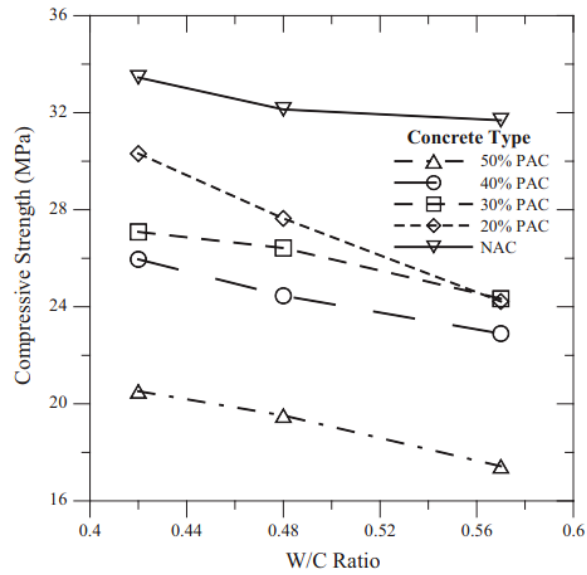


Fig.17 Concrete's compressive strength varies with the w/c ratio. Adapted from [Md. Jahidul Islam et al.,2016](#)

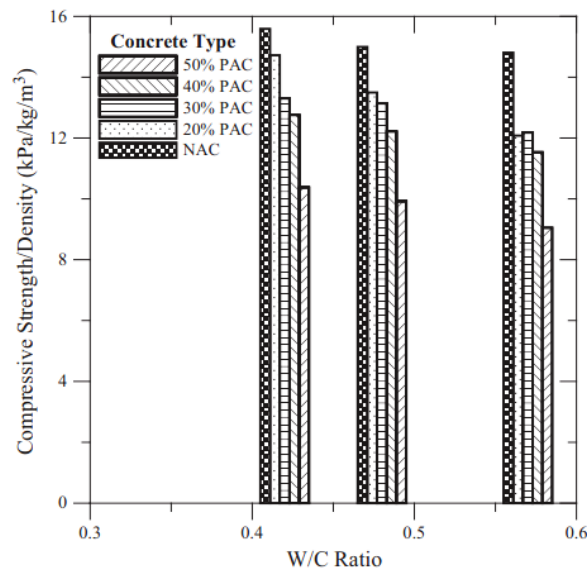


Fig.18 Changes in concrete's density and compressive strength with the w/c ratio. Adapted from [Md. Jahidul Islam et al.,2016](#)

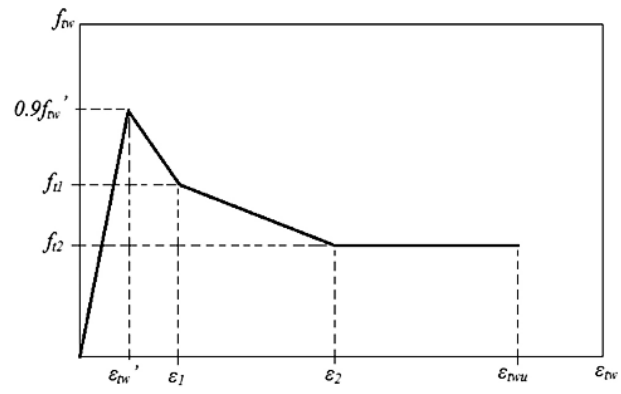


Fig.19 Proposed tensile stress-strain relationship for concrete made from recycled PET trash. Adapted from [Azad A. Mohammed 2017](#)